



Assessment of life cycle environmental impacts of materials, driving pattern, and climatic conditions on battery electric and hydrogen fuel cell vehicles in a cold region

Dipankar Khanna, Eskinder Gemechu, Nafisa Mahbub, Jubil Joy, Amit Kumar*

Department of Mechanical Engineering, Donadeo Innovation Centre for Engineering, University of Alberta, Edmonton, Alberta T6G 1H9, Canada



ARTICLE INFO

Keywords:

Battery electric vehicles
Hydrogen fuel cell vehicles
Life cycle assessment
Greenhouse gas emissions
Carbon fiber-reinforced plastic

ABSTRACT

Battery electric vehicles (BEVs) and hydrogen fuel cell vehicles (HFCVs) can play an important role in addressing climate change by diminishing greenhouse gas (GHG) emissions in the worldwide road transportation sector. There is limited research on the implications of the use of lightweight materials, driving pattern, and climatic impact on the life cycle GHG emissions in a cold region. To address this limitation, we developed a framework to assess eighteen BEV and four HFCV scenarios for a cold region that consider aforementioned parameters through a combination of driving patterns (in rural, city, and highway driving) and climatic conditions (i.e., summer, mild winter, and severe winter) for both conventional and carbon fiber-reinforced plastic (CFRP)-based BEVs. A case study was conducted for Canada, considering its cold regions, using available data for HFCVs. We assessed city driving in summer and highway driving in severe winter conditions for conventional and CFRP-based HFCVs. The results show that the lowest GHG emissions are in cities in summer, with life cycle GHG emissions values of 68.7 g CO₂ eq/km for CFRP-based BEVs. The highest life cycle GHG emissions are 364.4 g CO₂ eq/km with conventional HFCVs on the highway in severe winter conditions' scenario. The operation phase emerges as the primary contributor to life cycle GHG emissions, closely trailed by the production phase. The analysis shows that the most sensitive parameters for CFRP-based BEVs in the city in summer scenario are vehicle lifetime and for conventional HFCVs in the highway in severe winter scenario, fuel cell efficiency. The analysis also shows the range of life cycle GHG emissions for a cold region, with conventional HFCVs on highways in severe winter conditions exhibiting the highest emissions (331.0 g CO₂ eq/km) and CFRP-based HFCVs in the city in summer scenario the lowest (51.0 g CO₂ eq/km).

1. Introduction

The worldwide transportation sector significantly contributes to greenhouse gas (GHG) emissions, representing roughly 20 % of global emissions in 2021 (International Energy Agency, 2021; Koman et al., 2024). Road transportation is notably the main contributor to GHG emissions, accounting for a significant 72–75 % of emissions within the transportation sector (International Energy Agency, 2021; Koman et al., 2024). In 2018, most vehicles operating on the road worldwide were powered by gasoline and diesel (Kalghatgi, 2018; Wu et al., 2022). As a result of the ongoing expansion of the transportation sector, energy demand increased 9.3 % and GHGs increased 20 % between 2015 and 2020 (Environment Canada, 2014). In response to threats of climate change, governments worldwide are taking collective action. The

objective of the Paris Agreement is to limit the global temperature rise to below 2 °C above pre-industrial levels and to pursue efforts to further limit the temperature increase to 1.5 °C. (Cai et al., 2022; United Nations Climate Change, 2021). Achieving this target requires a transformation of the transportation sector for extensive decarbonization (Lefèvre et al., 2021; Shao et al., 2024). The primary approaches to decarbonize road transportation includes improving technology efficiency, transitioning to electrification, and adopting low-carbon fuels (Onat and Kucukvar, 2022; Smith and Huppmann, 2022). Battery electric vehicles (BEVs) and hydrogen fuel cell vehicles (HFCVs) are emerging as prominent choices (Smith and Huppmann, 2022; Zhang and Fujimori, 2020) as they offer significant reductions in GHG emissions compared to gasoline vehicles (Ellingsen et al., 2016; Smith and Huppmann, 2022).

BEVs distinguish themselves from conventional internal combustion

* Corresponding author.

E-mail address: Amit.Kumar@ualberta.ca (A. Kumar).

engine vehicles (ICEVs) by no carbon emissions during operation (Zhao et al., 2021). The environmental footprint of BEVs is contingent upon the source of electricity used to charge their batteries, whether it originates from renewable energy or a grid mix primarily powered by fossil fuels (Hawkins et al., 2013). It is noteworthy that renewable energy has the potential to decrease GHG emissions more than a low carbon electricity mix can. However, the amount depends on the source of the renewable energy (i.e., wind, solar, nuclear, hydro, etc.) (Doluweera et al., 2020; Marmiroli et al., 2018). Recent research by Andersson and Börjesson evaluated the impacts of renewable fuel use on the life cycle GHG performance of electric vehicles in the EU (Andersson and Börjesson, 2021). An LCA on BEVs in Germany found that GHG emissions associated with BEVs were 9–29 % lower than those of ICEVs in an average European Union (EU) electricity mix (Jochem et al., 2015). In Portugal, GHG emissions were 30–39 % lower, depending on the electricity mix and local climatic conditions (Garcia et al., 2015). Weis et al. and Onat et al. analyzed the effects of BEV charging cost on operation cost and GHG emissions in different states in U.S. (Onat et al., 2015; Weis et al., 2015). Their studies concluded that BEVs are the least energy-intensive options in 24 of 50 states, with lower GHG emissions when electricity is generated from low-emission sources (Onat et al., 2015; Weis et al., 2015).

In addition to the source of electricity, climate, road conditions, and driving patterns have an impact on a BEV's emissions, and vehicle and battery lifetime affect life cycle GHG emissions (Cox et al., 2020; Doluweera et al., 2020; Garcia et al., 2015; Hawkins et al., 2013; Ma et al., 2012). BEV batteries may need replacing several times, depending upon the driving patterns and climatic conditions of a geographic location (Burnham et al., 2006; Garcia et al., 2015; Glensor and María Rosa Muñoz, 2019; Hawkins et al., 2013; Hooftman et al., 2018; Koroma et al., 2022; Wang et al., 2008; Wong et al., 2021). Several other factors impact overall performance, i.e., battery efficiency, production, type and size; and driving range and conditions (Ellingsen et al., 2016). The energy consumed by auxiliary systems for heating and air conditioning (AC) also affects the energy efficiency of BEVs (Cox et al., 2020; Peters et al., 2017). In extreme cold weather, the auxiliary energy consumption increases up to 40 % from normal conditions (Faria et al., 2012, 2013). Moreover, the comprehensive life cycle of BEVs, encompassing the battery's life cycle, also contributes to the total GHG emissions of BEVs. Different batteries can be used in BEVs, i.e., lithium iron phosphate (LFP), nickel manganese cobalt (NMC), manganese cobalt oxide (MCO), and nickel cobalt oxide (NCO) (Matheys et al., 2009; Mayanti, 2024; Temporelli et al., 2020).

Hydrogen fuel is considered a more promising solution to address growing concerns of global warming than non-fossil energy sources (Bento, 2016; Egede et al., 2015; Onat et al., 2015; Wong et al., 2021). The fuel cell functions as an energy converter with an efficiency of 50 %, producing water vapour and heat as by-products (Candelaresi et al., 2021). A hydrogen fuel cell does not produce direct carbon emissions (Lee et al., 2018). Nonetheless, it is worth mentioning that HFCVs still produce notable GHG emissions, and the amount depends on the method used to produce hydrogen (Nikolaidis and Poullikkas, 2017). Basic methods of hydrogen production and the sources of hydrogen with percentage contributions are included in Section 1.2.1 of Supplementary Information file (SI).

In a U.S. study, the GHG emissions were 23 %, 14 %, and 1 % lower in hydrogen vehicles than in ICEVs when the hydrogen was produced from wind energy, natural gas, and coal gasification, respectively (Colella et al., 2005). Nigro and Jiang concluded that LCA results are affected by various input parameters such as vehicle type, climatic condition, geographic location, and resource availability (Nigro and Jiang, 2013). Fuel cell onboard storage is the most important component which contributes large increase in GHG emissions savings with a small improvement in fuel cell efficiency (Miotti et al., 2017; Simons and Bauer, 2015). Energy consumption is directly related to HFCV emissions. The energy consumed by the auxiliary system is for heating, air

conditioning, lighting, radio, and navigation, much of which depend on climatic conditions (Bauer et al., 2015).

Depending on the climatic conditions, heating and cooling system loads for HFCVs can increase energy consumption by up to 40 % compared to BEVs (Faria et al., 2012, 2013). The maintenance phase also contributes to GHG emissions. Replacing tires, the lead acid battery, windshield fluid, and engine oil generate 8.53 g CO₂ eq/km of GHG emissions. HFCVs have several disadvantages, such as challenges in tracking maintenance emissions for components like the fuel cell stack and powertrain system. In BEVs, stored electricity is the source of energy supply, while an HFCV uses a fuel cell to transform the stored hydrogen onboard the vehicle into electricity for the energy supply (Delucchi et al., 2014). The amount of energy recovered by regenerative braking affects the overall energy efficiency of both vehicles, particularly in downhill travel. Regenerative braking can recover 69 % of the energy through the components such as generator, controller, and the battery considered in HFCVs (De Vlieger et al., 2000; Egede et al., 2015). An aggressive driving style (sudden acceleration and breaking) leads to higher energy consumption whereas non-aggressive driving (smooth acceleration and breaking) results in a more efficient use of energy (De Vlieger et al., 2000). Road and climate conditions differ by geographical location.

In addition to road type and geographical location, vehicle size and weight affect energy efficiency. The energy required for driving is greater for large and heavy vehicles than for lighter and smaller vehicles because of increased rolling and air resistance (Egede et al., 2015; Jochem et al., 2015). Replacing conventional materials with lightweight alternatives reduces the weight of the vehicle, thereby improving energy efficiency and reducing GHG emissions. This is relevant for BEVs and HFCVs because the batteries, fuel cell, and additional electrical components make them heavier than similar ICEVs. A study by Czerwinski showed that a 10 % reduction in weight for a BEV increases its driving range by 13.7 %, and a 15 % reduction in the weight of a HFCV increases its driving range by 22 % (Czerwinski, 2021). Using lightweight materials like carbon fiber-reinforced plastic (CFRP) or glass fiber-reinforced plastic (GFRP) could enhance the energy efficiency of both BEVs and HFCVs (Patil et al., 2017). The manufacturing process and the physical specifications are given in Section 1.1 of the SI.

It is worth noting here that the few LCAs conducted assess the life cycle environmental impacts of the operation phase of BEVs and HFCVs (Ahmadi and Kjeang, 2015; Lee et al., 2018; Tagliaferri et al., 2016). During the operation phase, GHG emissions are influenced by factors such as driving pattern, road type, battery replacement, and climatic conditions (Greene, 2012; Tang et al., 2017). Furthermore, vehicle lifetime, as well as the durability of the battery in BEVs and the fuel cell in HFCVs, play an important role in overall life cycle emissions (Ahmadi and Kjeang, 2015; Burnham et al., 2006). Extreme weather conditions and aggressive driving patterns lead to frequent replacement of components, particularly tires and fluids, thus increasing overall GHG emissions (Bartolozzi et al., 2013; Dincer and Rosen, 2011; Hooftman et al., 2018; Huang and Zhang, 2006; Ma et al., 2012). One study considers replacing conventional materials with CFRPs to enhance vehicle efficiency and reduce environmental impact, even though CFRP is stronger and lighter than steel and aluminum (Osborne, 2013). The production of CFRPs, including asphaltene-based carbon fiber, is known to be energy and GHG emission-intensive (Koffler, 2014).

1.1. Perspective, novelty and objective

Although LCAs of various aspects such as driving pattern, road type, battery replacement, material and climatic conditions are separately available in existing literature, it cover specific scenarios. The combined effect of the aforementioned parameters on the LCA in a cold region is crucial for identifying the critical components and processes involved in evaluating the life cycle environmental impacts of conventional and CFRP-based BEVs and HFCVs in such regions. Furthermore, the life cycle

GHG emissions in every BEV and HFCV scenario assessed for this study were normalized based on the climatic and road conditions of two cities and compared in terms of environment impact using LCA. The base geographic location used for the normalization is Edmonton, and this city is compared with Vancouver. The Morris method was used to assess sensitivity by randomly varying one input parameter at a time to observe its impact on life cycle GHG emissions for different BEV and HFCV scenarios. The analysis helps to identify influential parameters on life cycle GHG emissions for both vehicles and provides the precautionary measures to reduce the environment impact. A Monte Carlo representation offers a thorough perspective on the probability distribution of the life cycle GHG emissions for each scenario. These analyses provide the information for policymakers and decision-makers on enhancing development of BEVs and HFCVs using life cycle assessment (LCA) for enhanced operational sustainability. Thus, it is imperative to assess the environmental advantages derived from a life cycle approach and bridge the aforementioned gaps through an LCA framework considering different parameters such as driving conditions and climate variations on the overall GHG performance of lightweight BEVs and HFCVs.

The specific aims of this paper include:

- Establishing an LCA framework for assessing both energy consumption and life cycle GHG emissions of conventional and CFRP-based BEVs and HFCVs over their entire life cycle.
- Calculating the impact of various driving patterns and climatic conditions on GHG emissions and energy consumption through an LCA of conventional and CFRP-based BEVs and HFCVs, by evaluating both the overall life cycle and individual phases of these vehicles.
- Determining the GHG emissions throughout the life cycle in various scenarios of BEVs and HFCVs based on the climatic and road conditions of two cities (Edmonton and Vancouver).
- Conducting detailed sensitivity and uncertainty analyses to identify and predict the crucial input parameters that significantly impact energy consumption and overall GHG emissions.

2. Method

We analyzed the environmental impacts of BEV systems through (LCA) following International Organization for Standardization (ISO) guidelines ([International Organization for Standardization 14040:2006, 2022](#)). According to ISO 14040:2006, LCA has four phases: goal and scope definition, life cycle inventory analysis, life cycle impact assessment, and interpretation of results ([International Organization for Standardization 14040:2006, 2022](#)).

2.1. Goal and scope definition

The main objective of this study is to assess and compare the GHG performance of lightweight (CFRP-based) BEVs and HFCVs with conventional (steel- and aluminum-based) BEVs and HFCVs ([Palazzo and Geyer, 2019](#)). 1 km is used as the functional unit and represents a measured performance of a product ([International Organization for Standardization 14040:2006, 2022](#)). A key aspect of carbon accounting is setting a time horizon to assess carbon impacts. The life cycle GHG emissions are expressed in terms of g CO₂ eq/km (GHG-100). A 100-year time horizon was adopted for the analysis. This choice of 100 years avoids distortions from longer time horizons that clash with social norms ([Fearnside, 2000](#)). We considered a mid-size five-seat passenger car with a lifetime of 200,000 km over an 11-year period for BEVs and a lifetime of 275,000 km over a 15-year period for HFCVs ([Argonne National Laboratory, 2018, 2022; Burnham et al., 2006; Chen et al., 2024; Peng et al., 2019](#)). Even though the distance of BEV and HFCV are different, average travelling distance for all the scenarios are conceded as 50 km per day ([Solar on EV, 2024](#)). Alberta, a Canadian province, is the base location for a case study and provides a real-world context for the study. It has a cold climate. Alberta's GHG emissions from gasoline

and diesel in the transportation sector are in Section 2.3.3 in SI file.

It is important to quantify the overall benefits of a reduction in environmental emissions by considering the entire life cycle, including extraction, vehicle manufacturing, assembly, vehicle operation, maintenance, and end of life. Fig. S1 in SI file shows the system boundary for carbon fiber production from asphaltene. Figs. 1 and Fig. S2 in SI file depict the system boundaries of BEVs and HFCVs, showing the life cycle stages and unit processes involved in the product systems. A detailed discussion of each life cycle stage, along with the data requirements, is given in Section 2 in the SI file.

2.2. Inventory analysis

2.2.1. Vehicle production

Two production pathways with different material characteristics were considered for the inventory analysis of the vehicle production phase. These pathways are BEVs and HFCVs constructed with steel and aluminum materials and (lightweight) BEVs and HFCVs constructed from asphaltene. Table S1 lists the primary vehicle components for both conventional and CFRP-based BEVs and HFCVs. Table S2 shows the mass percentage of the key raw materials for the main components of conventional and CFRP-based BEVs and HFCVs. The mass contribution of the primary raw materials in the two pathways is described in Section 2.1.1 in the SI. The mass conversion of different raw materials from conventional to CFRP for BEVs and HFCVs and the mass distribution of various components (conventional and CFRP-based BEVs and HFCVs) are listed in Tables S2 to S48 in the SI. This replacement reduces the total mass by 44 % ([Burnham et al., 2006; Czerwinski, 2021; Ghosh et al., 2021; Koffler, 2014; Wong et al., 2021](#)).

Table S3 lists the mass percentage and the key components of both conventional and CFRP-based lithium nickel manganese cobalt oxide (Li-NMC) batteries. Table S3 also gives the percentage mass distribution of hydrogen fuel cell onboard storage by principal raw materials for both conventional and CFRP-based HFCVs. The battery used in BEVs, its weight, capacity, efficiency, depth of discharge, and the number of battery replacements for the considered scenarios are described in Sections 2.3.3, 2.3.5, and 2.3.6 of the SI. The primary differences between HFCVs and BEVs are in the hydrogen fuel cell onboard storage and the powertrain system. The hydrogen fuel cell onboard storage system consists of its essential components, i.e., a compressed hydrogen tank system, fuel cell, water supply system, air supply system, cooling system, and piping system ([Burnham et al., 2006; Wang et al., 2008; Wong et al., 2021](#)). The emissions factor of the steam methane reforming (SMR) process, mass, capacity, pressure of the fuel cell onboard storage, and fuel cell efficiency are included in Section 2.3.6 in SI file. The GHG quantification of all materials used to manufacture the BEVs and HFCVs was calculated using the emission factors in Table S4 in the SI file ([Argonne National Laboratory, 2018; Burnham et al., 2006](#)). According to GREET (2018 model), the assembly stage includes paint production, vehicle component assembly, painting, heating, ventilation and air conditioning (HVAC), lighting, material handling, welding, and lithium-ion and lead-acid battery assembly. The primary energy consumption in these processes is electricity ([Argonne National Laboratory, 2018](#)). The energy use and greenhouse gas (GHG) emissions associated with each process are determined using data extracted from Burnham et al. ([Burnham et al., 2006](#)). There is more detail on the assembly in the SI, Section 3.1. Eq. 1 and Eq. 2 represent the production and assembly phase emissions for BEVs and HFCVs ([Argonne National Laboratory, 2018](#)).

$$\begin{aligned} \text{Production phase emission } & \left(\frac{\text{gCO}_2\text{eq}}{\text{km}} \right) \\ &= \sum \left(\text{Material for manufacturing (kg)} * \text{EF of material } \left(\frac{\text{gCO}_2\text{eq}}{\text{kg}} \right) \right) \\ &\quad / \text{Lifetime (km)} \end{aligned} \quad (1)$$

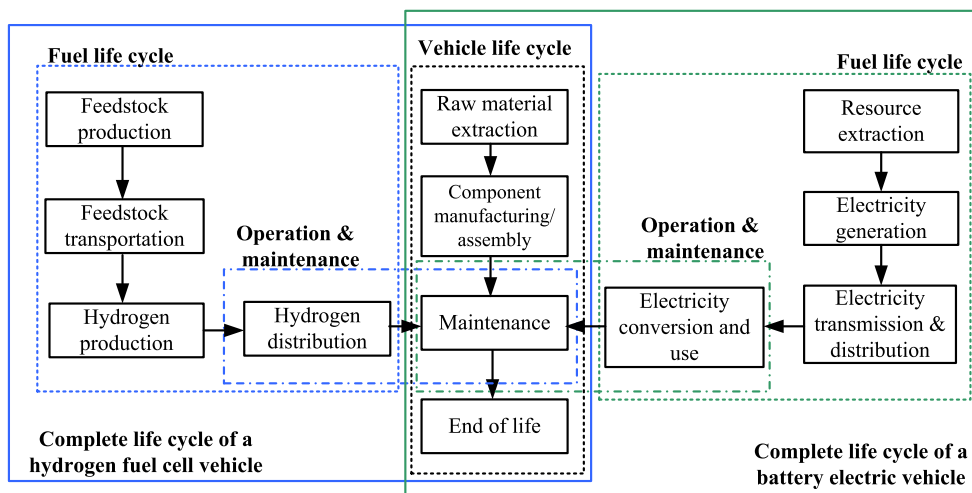


Fig. 1. System boundaries of the life cycle stages of hydrogen fuel cell and battery electric vehicles.

$$\text{Assembly phase emission } \left(\frac{\text{gCO}_2\text{eq}}{\text{km}} \right) = \frac{\left(\text{Energy for assembly (MJ)} * \text{EF of electricity grid mix } \left(\frac{\text{gCO}_2\text{eq}}{\text{MJ}} \right) \right)}{\text{Lifetime (km)}} \quad (2)$$

Where EF is the emission factor.

2.2.2. Vehicle operation and scenarios considered

The environmental performance during the operational phase is influenced by the composition of the grid mix in the region where the vehicle operates. The Low Emissions Analysis Platform (LEAP) model includes the dynamic GHG emission factors of Alberta's grid mix (Stockholm Environment Institute, 2022). Table 1 shows the GHG emission factors of the electricity grid mix for BEVs and HFCVs from 2020 to 2030 following LEAP modeling by our research group colleagues (Davis et al., 2020; Tao et al., 2011). Hydrogen is produced using the SMR process. Hydrogen production and transmission efficiency are included in Section 1.2.1 in the SI file.

The net energy requirement per km traveled is the sum of all the energy consumed during operation, which includes the energy for driving the wheels, air conditioning, heating, auxiliary, the energy dissipation (stopping at traffic signals, aggressive braking, and driving on uneven roads), and energy lost in the motor and controller (Egede et al., 2015; Tutuiu et al., 2015). Detailed information on all the considered energy consumption parameters for BEVs and HFCVs under their respective scenarios are in the SI in Section 2.3.2 (Table S52 and Table S53), Section 2.3.3 (Table S54 to Table S58), and Section 2.3.7 (Fig. S4). Factors such as driving patterns and climatic conditions influence the energy consumption of both BEVs and HFCVs. Driving patterns depend on the type of road (rural, city, highway) and prevalent climatic conditions (severe winter, mild winter, summer) (Doluweera et al., 2020). The temperature range for each climatic condition is shown in Table 2. With the road and climatic conditions assumed for vehicle operation in Alberta, we developed eighteen scenarios for BEVs and four for HFCVs. These are: rural in summer, rural in mild winter, rural in severe winter, city in summer, city in mild winter, city in severe winter, highway in summer, highway in mild winter, and highway in severe

Table 2
Temperature ranges in Alberta (Government of Canada, 2024a).

Scenario	Rural/City/Highway		
	Severe winter	Mild winter	Summer
Temperature range (°C)	-40.0 to -15.0	-14.0 to 14.0	15.0 to 35.0

winter for both conventional and CFRP-based BEVs and extreme operational scenarios such as city driving in summer and highway driving in severe winter for both conventional and CFRP-based HFCVs. Insufficient data is available for rural in summer, rural in mild winter, rural in severe winter, city in mild winter, city in severe winter, highway in summer, and highway in mild winter, so these scenarios were been included in the analysis. A bottom-up energy requirement model was developed for each scenario, and the equations used to determine the drag and rolling force are in Section 2.3.1 (SI). The calculation of production phase emission factor for BEV and HFCV is shown below.

Driving force for BEV and HFCV, DF (N)

$$= (0.5 * C_d * A * V^2 * P) + (C_r * m * g) \quad (3)$$

Where DF represents the driving force in Newton, while "C_d" and "C_r" denote the drag and rolling coefficients, respectively. The values of C_d and C_r for different scenarios are provided in Table S53 of the SI file. "A" represents the frontal area of BEV and HFCV, with the value of 2.27 m² (Nissan, 2019). "P" represents the density of air, and "g" represents the acceleration due to gravity, with values of 1.2 kg/m³ and 9.8 m/s², respectively (Nissan, 2019). "V" and "m" denote the speed and mass of the vehicle. The value of velocity for different scenarios are included in SI file Table S53. The total mass of conventional and CFRP-based BEV is 1511 kg and 877 kg, respectively, while the total mass of conventional and CFRP based HFCV is 1778 kg and 1000 kg, respectively. These values are represented in Table S1 and Table S2 in the SI file (Argonne National Laboratory, 2018; Burnham et al., 2006). The total operational phase energy for BEV and HFCV is given below.

$$\text{TE} = (((\text{DF (N)} * \text{Average distance per day (km)}) / 1000) (\text{MJ}) + \text{Auxiliary energy (MJ)}) \quad (4)$$

Table 1

GHG emission factors of Alberta's electricity grid mix for the considered years (from a study by our research group colleagues Davis et al. (Davis et al., 2020)).

Operational year	2020	2021	2022	2023	2024	2025	2026	2027	2028	2029	2030
Emission factors (g CO ₂ eq/MJ)	151.0	141.0	134.0	110.0	114.0	122.0	117.0	113.0	100.0	92.0	85.0

$$\text{Operational phase emissions for BEV} \left(\frac{\text{gCO}_2\text{eq}}{\text{km}} \right) = \frac{\left(\text{TE (MJ)} * \text{EF of electricity grid mix} \left(\frac{\text{gCO}_2\text{eq}}{\text{MJ}} \right) \right)}{\text{Lifetime (km)}} \quad (5)$$

Average distance per day for BEV and HFCV is 50 km per day (Solar on EV, 2024). Auxiliary energy values are included in Table S52 of the SI file (Brodrick et al., 2002; De Vlieger et al., 2000; Milligan, 2017; Tutuiu et al., 2015).

$$\text{Operational phase emissions for HFCV, } \left(\frac{\text{gCO}_2\text{eq}}{\text{km}} \right) = \frac{\left(\frac{\text{TE (MJ)}}{\text{LHV} \left(\frac{\text{MJ}}{\text{kg}} \right)} \right) * \text{EF of hydrogen} \left(\frac{\text{gCO}_2\text{eq}}{\text{kg}} \right)}{\text{Lifetime (km)}} \quad (6)$$

Lower heating value (LHV) of hydrogen is 120 MJ/kg, and the emission factor is 9.17 kgCO₂eq/kg of hydrogen (Ebaid et al., 2015; Oni et al., 2022).

During the operation of the vehicle, tires, fluids, batteries and fuel cells degrade over time; periodic maintenance or replacement is required to sustain vehicle efficiency and fuel economy. In this analysis, the tires, brake fluid, and powertrain coolant are replaced three times during the entire life cycle of BEVs and HFCVs. The details on maintenance intervals and number of replacements of materials and components are included in Section 2.4 (Table S59 and Table S60) in the SI. The emissions during the maintenance phase are calculated using the following equation. Energy for the maintenance phase is not quantified because its contribution is very small compared to other life cycle phases. Emission values for the maintenance phase are directly sourced from the literature for emission calculations (Argonne National Laboratory, 2018; Bartolozzi et al., 2013; Hawkins et al., 2013).

$$\text{Maintenance phase emission} = \sum \text{Emission of all replaced components} \quad (7)$$

A number of replacements of the components and corresponding emission values are included in Table S59 and S60 in the SI file.

The recycling phase is omitted from this study. Only disposal is examined in the end-of-life phase. The disposal phase of a vehicle includes sorting or dismantling, shredding, transportation, and landfilling or disposal. All these phases involve energy consumption and associated GHG emissions. Detailed calculations for energy consumption and GHG emissions are described in Section 2.5 (Table S61 to Table S72) in the SI. The emissions during the end-of-life phase are calculated using the following equation: (Bakker, 2010; Kukreja, 2008; Nemry et al., 2008; Staudinger et al., 2001).

$$\text{End - of - life phase emissions} = \sum \text{Energy required for disposal}^* \text{ Emission factor} \quad (8)$$

The total life cycle emissions for BEV and HFCV are the sum of emissions from the production, assembly, operation, maintenance, and end-of-life phases.

2.2.3. Normalization of the life cycle GHG emission

The life cycle GHG emissions in every BEV and HFCV scenario were normalized based on the climatic and road conditions of two cities: Edmonton, Alberta, and Vancouver, British Columbia. The average GHG

emissions from all the considered scenarios provide the normalized values for the considered pathways (i.e., conventional and CFRP-based BEVs and HFCVs). Edmonton serves as the base geographic location for normalization, and the results are compared those with Vancouver. In the normalization, severe and mild winter climates are compared. Edmonton is one of the cities in Alberta province, which is considered as the cold region in the analysis. On the other hand, Vancouver, situated in British Columbia province, represents the mild winter region in this analysis. Table 3 shows the percentage variation in road type and climatic conditions of Edmonton and Vancouver for all the scenarios. Furthermore, Eq. 9 represents the method used to calculate the normalized GHG emissions in both cities.

CC is the climatic conditions, which transition from severe winter (a) to summer (c). RT stands the road type, transitioning from highway (i) to rural (k). Each combination of CC and RT yields nine scenarios, and summing up all scenarios provides the normalized value for each particular city.

2.2.4. Sensitivity analysis

To avoid any misleading conclusions in an LCA-based decision, the results need to be evaluated through sensitivity and uncertainty analyses. The Regression, Uncertainty, and Sensitivity Tool (RUST) model, an Excel-based tool developed by our research group colleagues Di Lullo et al. (Di Lullo et al., 2020), was used in this study. A sensitivity analysis, as described by Campolongo et al. and Wager et al., was conducted to identify the key parameters that have a significant impact on the model output (Campolongo et al., 2007). Morris's statistical method was implemented for this purpose. The Morris method identifies important parameters from a high number of model inputs. Once the key sensitive input parameters were identified, an uncertainty analysis was run using a Monte Carlo simulation to provide the likely range of life cycle GHG emissions for each scenario for both CFRP and conventional BEVs and HFCVs. Table 4 shows the maximum and minimum range of input parameters for the sensitivity analysis of BEVs and HFCVs.

The prime limitation of this study is that the framework for the LCA of BEVs and HFCVs is based on data from published literature. Additionally, composite materials (other than CFRP), future technologies (such as exhaust gas recirculation [EGR]), and new energy vehicle (NEV)]technology including renewable energy are not considered in this study. This study does not include comprehensive details of different types of advanced batteries, and lightweight materials are not evaluated. All the inventory data related to raw material extraction and vehicle components was derived from a single database for mid-size vehicles (From GREET 2018 model). Furthermore, an uncertainty analysis of the various data collected from other articles has not been conducted in this current research. Another limitation is that the recycling phase assumptions are based on current technologies. This is due to the lack of reliable information on future technologies, i.e., open loop, closed loop, hydrometallurgy, and pyrometallurgy.

3. Results and discussion

This section presents the GHG emissions estimation of conventional and CFRP-based BEVs and HFCVs. The GHG emissions are evaluated in g CO₂ eq per km, assuming a lifetime of 200,000 km for BEVs and 275,000 km for HFCVs (Argonne National Laboratory, 2018, 2022; Burnham et al., 2006; Chen et al., 2024; Peng et al., 2019). HFCVs have more emissions per vehicle than that of BEVs because of the higher lifetime. The extended lifetime of HFCV is due to the reduced maintenance or less replacement of fuel cells when compared to batteries in BEV. The

Table 3

Percentage variation in road type and climatic conditions of Edmonton and Vancouver (Government of Canada, 2021, 2024b; Statistics Canada, 2009, 2019).

$$\text{Normalized GHG emissions in a city} = \sum_{CC}^{CC(c), RT(k)} (life cycle emissions * CC * RT)$$

(9)

Climatic conditions (CC)	Edmonton (%)	Vancouver (%)	Road type (RT)	Edmonton (%)	Vancouver (%)
Severe winter (a)	50	15	Highway (i)	50	45
Mild winter (b)	30	55	City (j)	35	35
Summer (c)	20	30	Rural (k)	15	20

Table 4

Values for sensitive parameters of BEVs and HFCVs.

Parameter	BEV and HFCV	
	Min. to Max. value	
Acceleration, a (m/s ²) (Egede et al., 2015; Giordano et al., 2023)	0.100–0.400	
Battery efficiency, η (%) (Burnham et al., 2006; Del Duce et al., 2016; Egede et al., 2015; Milligan, 2017)	81.00–90.00	
Distance (km/day) (Doluweera et al., 2020)	80.00–20.00	
Drag coefficient, C _d (Amasawa et al., 2020)	0.200–0.520	
Efficiency of fuel cell (%) (Candelaresi et al., 2021)	30.00–60.00	
Emission factor of hydrogen (g CO ₂ eq/kg) (Oni et al., 2022)	8.00–14.00	
Frontal area, A (m ²) (Nissan, 2019)	1.50–3.50	
Mass of BEV (kg) (Argonne National Laboratory, 2018; Burnham et al., 2006; Wong et al., 2021)	789.0–1750	
Mass of HFCV (kg) (Argonne National Laboratory, 2018; Burnham et al., 2006; Wong et al., 2021)	700.0–1956	
Motor & controller efficiency (%) (Müller et al., 2020)	75.00–95.00	
Power rating of AC (kW) (Wager et al., 2016)	1.00–2.50	
Power rating of heater (kW) (Wager et al., 2016)	1.00–3.50	
Rolling coefficient, C _r (Müller et al., 2020)	0.0024–0.7600	
Speed (km/h) (Giordano et al., 2023)	30.00–55.00	

Note: The battery efficiency is shown for BEVs only. The fuel cell efficiency and hydrogen emission factor are shown for HFCVs only. BEV and HFCV lifetimes range from 100,000–220,000 and 200,000–350,000 km, respectively (Ahmadi and Kjeang, 2015; Hawkins et al., 2013).

average daily travelling distance for all the scenarios for BEVs and HFCVs is assumed to be 50 km per day (Solar on EV, 2024). Battery replacement in BEVs occurs at a specific kilometer threshold, establishing a uniform basis for comparing BEVs and HFCVs. Consequently, GHG emissions are evaluated in g CO₂ eq per km ensuring a consistent assessment across both vehicle types (Canada energy regulator, 2022; Chen et al., 2024). First, the GHG emissions generated from the vehicle component production are discussed, followed by the operational emissions in eighteen BEV and four HFCV scenarios, and the base case is analyzed for Alberta, Canada. The individual descriptions of the life cycle phases, except production and operation, are not included in this section. However, these life cycle stages are accounted for in the total life cycle GHG emission. The climatic and road conditions and the driving behaviors are normalized with reference to Edmonton, Alberta, and Vancouver, British Columbia, to understand the overall GHG emission performances of conventional and CFRP-based BEVs and HFCVs. Finally, the sensitivity analysis results are discussed.

3.1. Vehicle production GHG emissions

Fig. 2 shows the production GHG emission contributions from the critical raw materials of BEVs and HFCVs. Steel and aluminum are the materials with high GHG contributions: their emissions are 44 % and 19.6 %, respectively, in conventional BEVs and 45 % and 7 %, respectively, in conventional HFCVs. The high GHG emissions from these materials are due to their large mass contributions and energy-intensive manufacturing processes. Plastic, rubber, and copper also have significant GHG emissions contributions in conventional BEVs and HFCVs. In

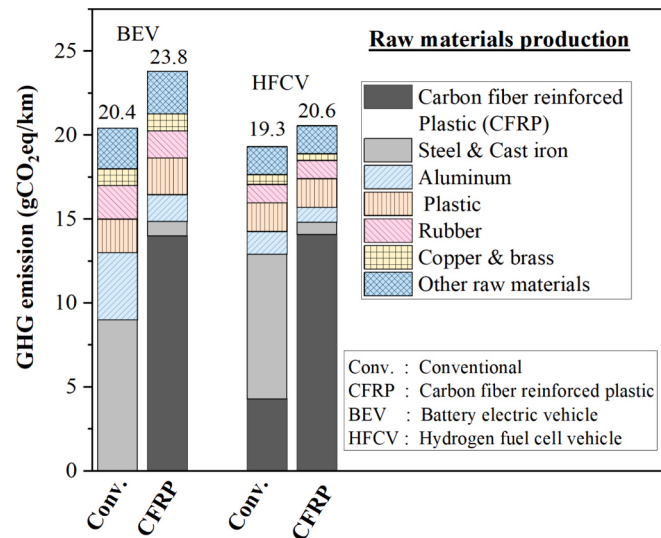


Fig. 2. GHG emissions contribution by raw materials for both conventional and CFRP-based BEVs and HFCVs.

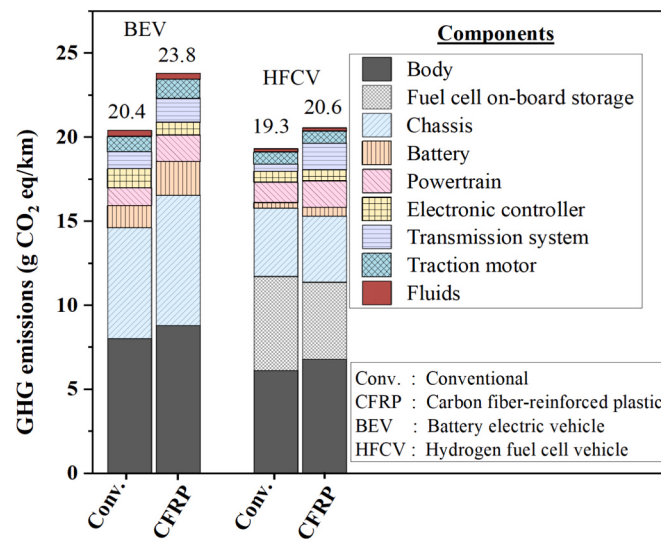


Fig. 3. GHG emissions contribution by critical components for both conventional and CFRP-based BEVs and HFCVs.

CFRP-based BEVs and HFCVs, the most significant contribution is from carbon fiber, which makes up around 69 % of the production emissions in BEVs and 73 % in HFCVs. Carbon fiber production involves a series of energy-intensive processes that result in higher GHG emissions per kg of carbon fiber than from conventional raw materials.

Fig. 3 shows the GHG emissions from the key components generated during BEV and HFCV production. The total GHG emissions from

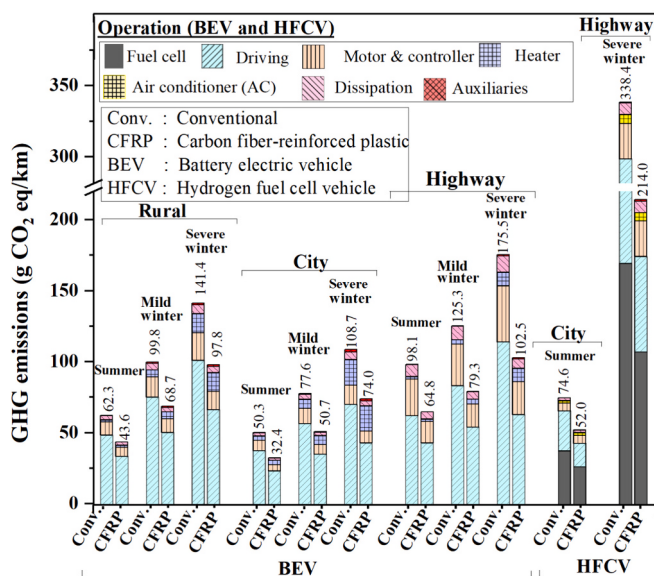


Fig. 4. GHG emissions contribution during the operation phase for both conventional and CFRP-based BEVs and HFCVs, all scenarios.

conventional BEVs are 12.4 % lower than those of CFRP-based BEVs. In both conventional and CFRP-based BEVs, the highest GHG emissions are from the production of the body and the chassis, which together account for more than 76 % of vehicle production emissions. A conventional HFCV generates 9.3 % fewer GHG emissions than a CFRP-based HFCV. Similar to a BEV, the highest GHG emissions in both types of HFCV are due to the fabricating of the body and the chassis, which together account for almost 55 % of the vehicle's production phase emissions.

3.2. Operation phase GHG emissions

Fig. 4 shows the GHG emission results for every scenario. CFRP-based BEVs generate 36–42 % fewer operational GHG emissions than conventional BEVs. The highest operational phase GHG emissions are observed in the highway in severe winter scenario for conventional BEVs, 176 g CO₂ eq/km, and the lowest in CFRP-based BEVs in the city in the summer scenario, 32.4 g CO₂ eq/km. CFRP-based HFCVs emit 37 % and 42 % fewer operational GHG emissions in the city during summer and on highways during severe winter scenarios than corresponding conventional HFCVs. The highway in severe winter scenario shows the highest GHG emissions for both conventional and CFRP pathways at 338 g CO₂ eq/km for a conventional HFCV and 214 g CO₂ eq/km for a CFRP-based HFCV. In the city in summer scenario, a conventional HFCV emits 75 g CO₂ eq/km, whereas a CFRP-based HFCV emits 52 g CO₂ eq/km. The highest GHG emissions reduction in CFRP-based BEVs and HFCVs compared to conventional BEVs and HFCVs is seen in the highway in severe winter scenarios.

The operational GHG emissions associated with driving BEVs range from 58 to 78 % for all scenarios. In HFCVs, the primary contributor of operational GHG emissions is the fuel cell, which is 50 % in all CFRP and conventional vehicle scenarios. Additionally, the operational GHG emissions associated with driving HFCVs range from 31 to 38 % for all scenarios. The reduction in operation GHG emissions observed in both CFRP-based BEVs and HFCVs may be due to their lower mass. The factors mentioned above are less significant if the vehicle mass is low, given that low mass lowers driving energy. A CFRP-based BEV has 42 % less mass than a conventional BEV. Similarly, a CFRP-based HFCV weighs 44 % less than a conventional HFCV. The lower mass reduces drag and rolling resistance, leading to improved energy efficiency. The lightweight construction of CFRP-based vehicles reduces the total energy demand for a given distance compared to conventional BEVs and HFCVs.

This reduction in energy significantly reduces the operational phase GHG emissions of the vehicles, as shown below in Fig. 4. The detailed operation energy consumption data for in every category (driving, AC and heaters, auxiliaries, dissipation energy, and energy lost in the motor and controller) is in Section 3.2 (Table S74 to Table S109) in the SI. Furthermore, the higher fuel efficiency in cities compared to highways due to the country-specific reason. The driving pattern in city is calm, the traffic jams and congestion are not significantly impacting fuel efficiency. In contrast, the driving range on highways is lower due to aggressive driving. Additionally, lower motor and controller efficiency, higher speeds and acceleration, and increased rolling and drag forces on highways decreases the fuel efficiency, resulting in lower fuel efficiency on expressways compared to cities.

3.3. Life cycle GHG emissions

Fig. 5 shows the net life cycle GHG emissions for both conventional and CFRP-based HFCVs and BEVs. The life cycle GHG emissions of CFRP-based BEVs range from 68.65 g CO₂ eq/km in the city in summer to 148.57 g CO₂ eq/km on the highway in severe winter scenarios. A conventional BEV generates higher emissions, from 86.0 to 233.45 g CO₂ eq/km among the assessed scenarios. For the eighteen BEV scenarios evaluated, the highest GHG emissions are in the highway in severe winter scenario when CFRP replaces conventional materials. Operation phase emissions make the highest contribution to the total emissions, from 47 % for a CFRP-based BEV in the city in summer to 71 % for a conventional BEV on the highway in severe winter conditions.

Production phase GHG emissions contribute 12 % for a conventional BEV on a highway in severe winter and up to 33 % for a CFRP-based BEV in a city in summer. The remaining life cycle stages, such as assembly, maintenance, and end of life, make up less than 10 % of life cycle GHG emissions in every BEV scenario. The GHG emissions for the assembly and end-of-life phases in the conventional and CFRP-based BEV scenarios are shown in Table S73 and Table S109, respectively, in the SI. GHG emissions depend significantly on road patterns and the prevailing climatic conditions and are higher on highways in severe winter given the increased energy requirements at higher speeds; the increase is directly proportional to factors like acceleration, drag force, frontal area, etc. BEVs also consume more energy in severe winter conditions than in summer to maintain the battery's thermal chemistry than in summer, thus more GHGs are emitted on the highway in severe winter

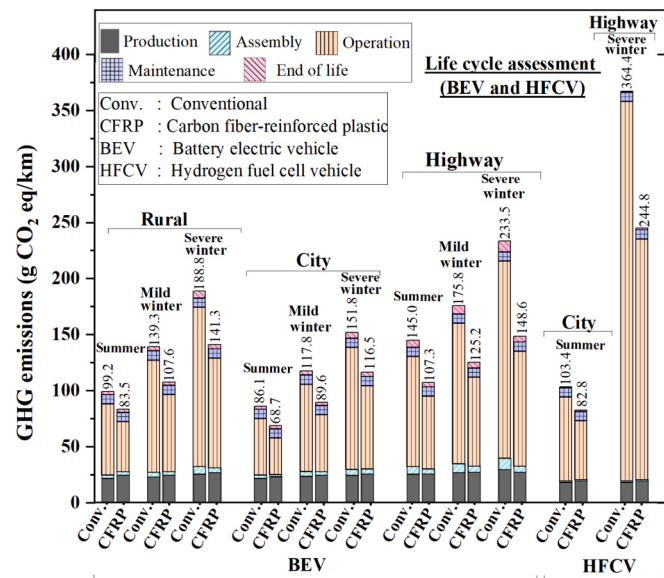


Fig. 5. Life cycle GHG emissions contribution for both conventional and CFRP-based BEVs and HFCVs, all scenarios.

conditions than in the city in summer.

The highest life cycle GHG emissions for conventional and CFRP-based HFCVs are on the highway in severe winter conditions, 367 g CO₂ eq/km, and 244 g CO₂ eq/km, respectively. Conventional HFCVs emissions are 26 % higher in the city in summer and 50 % higher on the highway in severe winter conditions than CFRP-based HFCVs. As for BEVs, in every HFCV scenario, operation phase emissions make the largest contribution, 64 % to 92 %, followed by production phase GHG emissions of 4 % to 23 % of the total, and the contributions from other life cycle phases, i.e., assembly, maintenance, and end of life, are less than 10 %.

Production phase GHG emissions are consistently higher for CFRP-based BEVs and HFCVs than for conventional BEVs and HFCVs in every scenario, primarily because of the high emissions intensity of CFRP processing compared with steel and aluminum. In both BEVs and HFCVs, however, the operation phase emits the most life cycle GHGs of all the phases throughout the vehicle's life. As noted above, the key parameters influencing the operational phase GHG emissions are road type, climatic conditions, and driving patterns.

The normalized GHG emissions of conventional and CFRP-based BEVs and HFCVs are presented in Fig. 6. BEVs and HFCVs emit fewer GHGs in Vancouver than in Edmonton, likely because of Vancouver's lower grid GHG emissions intensity, which averages 40 g CO₂ eq/kWh. This lower intensity is due to the higher contribution of clean energy sources like hydropower than in Alberta's mixed electricity grid. Moreover, Vancouver's short winters and long summers result in lower operational GHG emissions than in Edmonton. In Edmonton, both BEVs and HFCVs in the conventional pathway generated 28 to 32 % more life cycle GHG emissions than in the CFRP pathway. However, in Vancouver, conventional BEVs emit only 6 % more life cycle GHGs than CFRP-based BEVs. Yet in HFCVs, the CFRP pathway produced 21 % more GHG emissions than in the conventional pathway; this is due to the increased energy consumption and longer vehicle lifetime. The material choice is the key factor affecting GHG emissions in BEVs and HFCVs (Canadian Automobile Association: Alberta Motor Association, 2024; Travel British Columbia, 2024). As mentioned earlier, CFRP-based HFCVs emit more life cycle GHGs than conventional HFCVs largely because CFRP is more energy-intensive than materials like steel and aluminum.

3.4. Sensitivity and uncertainty

Fig. 7 shows the sensitivity analysis results of CFRP-based BEVs in the city in summer scenario and Fig. 8 the results for conventional HFCVs on the highway in severe winter conditions in Edmonton,

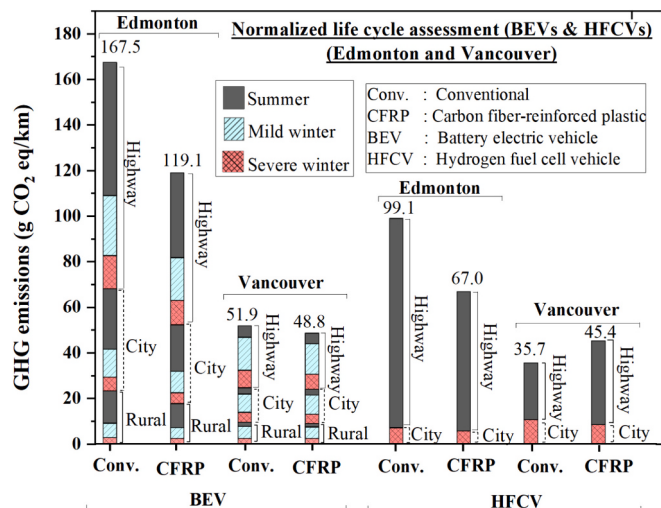


Fig. 6. Normalized life cycle GHG emissions contribution for both conventional and CFRP-based BEVs and HFCVs, all scenarios.

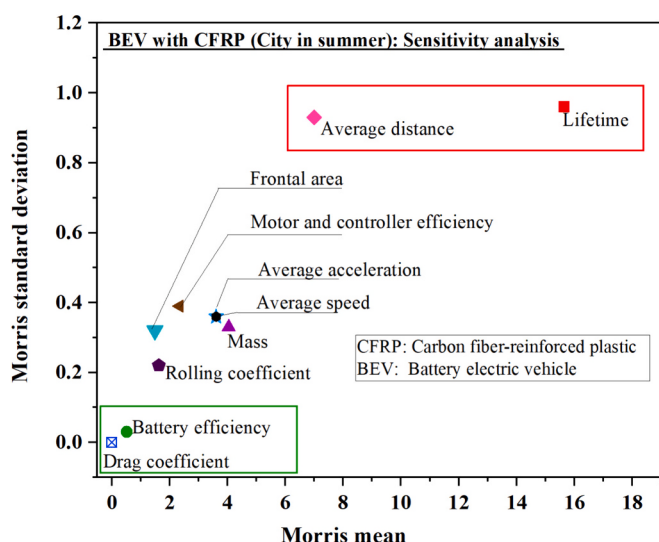


Fig. 7. Sensitivity analysis for life cycle GHG emissions in CFRP-based BEVs (city in summer).

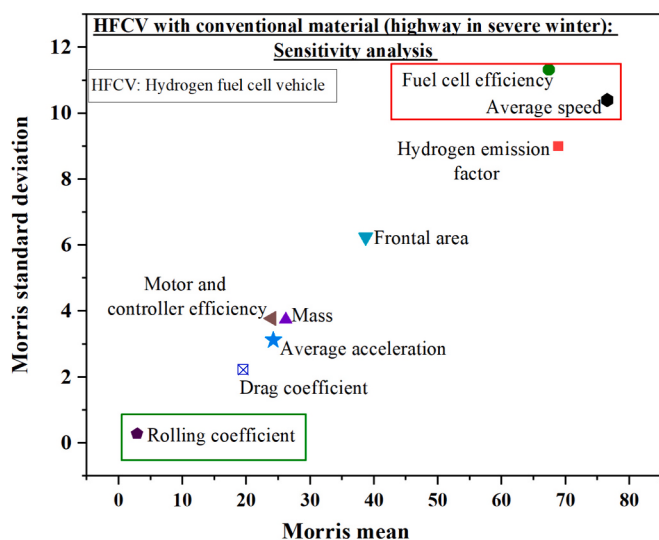


Fig. 8. Sensitivity analysis for life cycle GHG emissions in conventional HFCVs (highway in severe winter).

Alberta. In the sensitivity analysis of a CFRP-based BEV in the city in the summer scenario, the parameters that significantly influence the life cycle GHG emissions are vehicle lifetime and average distance traveled (shown in the red box in Fig. 7). On the other hand, for a conventional HFCV in the highway in severe winter scenario, the sensitivity analysis shows that the key parameters that influence life cycle GHG emissions are fuel cell efficiency, average speed, hydrogen emission factor, and frontal area. Lifetime refers collectively to the phases of the vehicle's life cycle, i.e., production, assembly, operation, maintenance, and end of life. Detailed explanation is included in the Section 3.4 of the SI file.

In both Fig. 7 and Fig. 8, the parameters in the green box are considered to have the least effect on life cycle GHG emissions. This is based on their small mean and standard deviation values. The parameters between the red and green boxes in the two figures are categorized as moderately significant in terms of their impact on life cycle GHG emissions. Sensitivity analysis results of the remaining seventeen BEV and three HFCV scenarios are in Section 3.4 (Fig. S5 to Fig. S24) in the SI.

Fig. 9 is a box plot that shows the range of life cycle GHG emissions

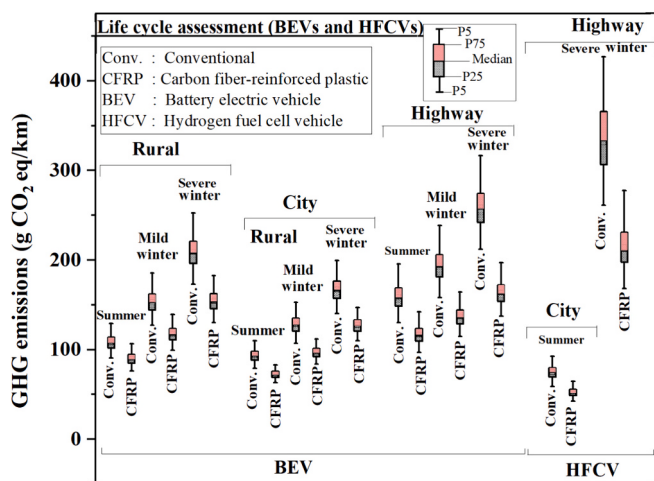


Fig. 9. Uncertainty analysis for life cycle GHG emissions in both conventional and CFRP-based BEVs and HFCVs, all scenarios.

for all scenarios, i.e., both CFRP and conventional BEVs and HFCVs. The Monte Carlo simulation shows the highest value of mean life cycle GHG emissions in the conventional HFCV in the highway in severe winter conditions (331 g CO₂ eq/km). The most likely life cycle GHG emissions range from 261 to 427 g CO₂ eq/km for that scenario. The lowest mean life cycle GHG emissions of 51 g CO₂ eq/km are achieved in a CFRP-based HFCV in the city in summer scenario (for Edmonton, Alberta). The most likely life cycle GHG emissions for this scenario are between 47.1 and 65 g CO₂ eq/km.

For BEVs, the highest mean life cycle GHG emissions (257 g CO₂ eq/km) are in conventional vehicles on the highway during severe winter conditions and the lowest mean life cycle GHG emissions (72 g CO₂ eq/km) are in CFRP-based vehicles in the city in summer scenario. The most likely life cycle GHG emissions ranges for all seasons and scenarios for both conventional and CFRP-based BEVs are 63–199 g CO₂ eq/km for city driving, 76–252 g CO₂ eq/km for rural driving, and 97–317 g CO₂ eq/km for highway driving. These values provide insight into the expected GHG emissions for different driving conditions and materials.

4. Potential for future research

NEVs have been growing rapidly because of the potential to reduce GHG emissions and use clean energy (Li et al., 2024). The framework developed for materials, driving patterns, and climatic conditions could be applied to NEVs under various operational conditions. Compared to conventional vehicles, NEVs can be operated using clean energy such as wind and solar power to provide energy resources and reduce environmental pollution (Zheng et al., 2018). Current research on NEV is focused on policy, environmental impact, operating technologies, and consumer purchase factors (Li et al., 2024). To encourage individuals or institutions to purchase NEVs, governments introduced policies that are suitable for the development of NEVs. Environmental policies are expected to reduce GHG emissions and financial subsidy-based policies are most common (Zhang and Qin, 2018). Reduced purchase price, subsidies, tax credits, longer vehicle warranties, and rebates on vehicle registration are the incentives or financial subsidy policies (Lu et al., 2022). The prime challenges of NEV are battery charging stations, battery swapping, hydrogen production from renewable energy sources, and hydrogen refueling stations (Mohammed et al., 2024). In addition to the design improvement of battery, fuel cell, lightweight material, and charging infrastructure, vehicle to grid (V2G) technology provides energy saving by bi-directional charging, which makes it possible to charge the EV battery and utilize the energy stored in the car's battery and push it back to the power grid (Ghirardi et al., 2024; Kwon et al., 2020). The development of policy using the aforementioned NEV concept with

renewable energy may be an area for future research.

5. Conclusion

This study compared the life cycle GHG emissions of carbon fiber-reinforced plastic (CFRP)-based battery electric vehicles (BEVs) and hydrogen fuel cell vehicles (HFCVs) with conventional and BEV and HFCV pathways in a cold climate like Canada's. In every scenario assessed, substituting steel, aluminum, and other conventional raw materials with CFRP in the key components of BEVs and HFCVs reduces GHG emissions considerably, especially in the operation phase. Based on climatic and driving conditions, eighteen operational scenarios for BEVs and four for HFCVs were analyzed. Among them, the lowest GHG emissions are in the city in summer scenario, with life cycle GHG emissions values of 86.1 g CO₂ eq/km for conventional BEVs and 68.7 g CO₂ eq/km for CFRP-based BEVs. The life cycle GHG emissions are highest for conventional HFCVs (364.4 g CO₂ eq/km) and CFRP-based HFCVs (244.8 g CO₂ eq/km) in the highway in severe winter scenario. In every BEV and HFCV scenario, the greatest GHG emissions are in the operation phase, 47–71 % for BEVs and 64–92 % for HFCVs. The production phase is the next highest contributor to life cycle GHG emission; it makes up 12–33 % of the total emissions for BEVs and 4–23 % for HFCVs in all scenarios. In conventional and CFRP-based BEVs and HFCVs, the highest production GHG emissions are due to the fabrication of the body and the chassis. The contributions from other life cycle phases, such as assembly, maintenance, and end of life, are less than 10 % in all BEV and HFCV scenarios.

The parameters that significantly influence life cycle GHG emissions in CFRP-based BEVs in the city in summer scenario are lifetime and average distance traveled. In a conventional HFCV on highways during severe winter conditions, the parameters influencing life cycle GHG emissions are fuel cell efficiency, average speed, hydrogen emissions factor, and frontal area. These parameters should be carefully evaluated to improve overall GHG emission reduction. The uncertainty analysis shows that the highest and lowest mean life cycle GHG emissions are 331 g CO₂ eq/km and 51 g CO₂ eq/km, respectively. These values correspond to a conventional HFCV on a highway during severe winter conditions and a CFRP-based HFCV in the city during the summer. The results of this study can help stakeholders and policymakers in determining the suitability of manufacturing CFRP-based BEVs and HFCVs in a cold climate globally.

CRediT authorship contribution statement

Dipankar Khanna: Conceptualization, Methodology, Investigation, Formal analysis, Validation, Writing – original draft. **Eskinder Gemechu:** Methodology, Data curation, Validation, Writing – review & editing. **Nafisa Mahbub:** Methodology, Data curation, Validation, Writing – review & editing. **Jubil Joy:** Methodology, Data curation, Validation, Writing – review & editing. **Amit Kumar:** Conceptualization, Methodology, Supervision, Resources, Funding acquisition, Validation, Writing – review & editing.

Declaration of competing interest

None.

Data availability

Data will be made available on request.

Acknowledgements

The authors are thankful to Alberta Energy and Minerals (AEM), Natural Resources Canada (NRCan), the U.S. Department of Transportation Federal Highway Administration, and the National Household

Travel Survey of Alberta for providing the relevant data to execute this research successfully. The authors would like to acknowledge the support of Natural Sciences and Engineering Research Council of Canada (NSERC) Alliance Grant Project on Integrated Assessment of Energy Systems and the Cenovus Energy Endowed Chair Program in Environmental Engineering for funding the research project. The authors are grateful to representatives from Cenovus Energy Inc., Suncor Energy Inc., Alberta Innovates, Natural Resources Canada (NRCan), Alberta Energy and Minerals (AEM) and Environment and Climate Change Canada (ECCC) for their inputs and comments during the course of this study. As a part of the University of Alberta's Future Energy Systems (FES) research initiative, this research was made possible in part thanks to funding from the Canada First Research Excellence Fund (CFREF). This research was undertaken, in part, thanks to funding from the Canada Research Chairs Program. This funding was provided in support of the Canada Research Chair in Assessment of Energy Systems (Tier-1). The authors thank Astrid Blodgett for editing this paper. The authors are obliged to Future Energy Systems (FES) for providing funding from the Canada First Research Excellence Fund. We thank Astrid Blodgett for editing this paper and acknowledge Abayomi Olufemi Oni from the University of Alberta for providing valuable input and feedback throughout the research.

Appendix A. Supplementary data

Supplementary data to this article can be found online at <https://doi.org/10.1016/j.eiar.2024.107680>.

References

- Ahmadi, P., Kjeang, E., 2015. Comparative life cycle assessment of hydrogen fuel cell passenger vehicles in different Canadian provinces. *Int. J. Hydrol. Energy* 40, 12905–12917. <https://doi.org/10.1016/j.ijhydene.2015.07.147>.
- Amasawa, E., Hasegawa, M., Yokokawa, N., Sugiyama, H., Hirao, M., 2020. Environmental performance of an electric vehicle composed of 47% polymers and polymer composites. *Sustain. Mater. Technol.* 25, e00189. <https://doi.org/10.1016/j.susmat.2020.e00189>.
- Andersson, Ö., Börjesson, P., 2021. The greenhouse gas emissions of an electrified vehicle combined with renewable fuels: life cycle assessment and policy implications. *Appl. Energy* 289, 116621. <https://doi.org/10.1016/j.apenergy.2021.116621>.
- Argonne National Laboratory, 2018. The Greenhouse Gases, Regulated Emissions, and Energy Use in Transportation Model (GREET). <https://greet.anl.gov> (accessed 18 March 2020).
- Argonne National Laboratory, 2022. Cradle-to-grave lifecycle analysis of U.S. light-duty vehicle-fuel Pathways: A greenhouse gas emissions and economic assessment of current (2020) and future (2030–2035) technologies <https://www.osti.gov/biblio/1875764> (accessed 18 March 2023).
- Bakker, D., 2010. Battery Electric Vehicles. https://www.academia.edu/30578520/Battery_Electric_Vehicles_Performance_CO_2_emissions_lifecycle_costs_and_advanced_battery_technology_development (accessed 5 November 2023).
- Bartolozzi, I., Rizzi, F., Frey, M., 2013. Comparison between hydrogen and electric vehicles by life cycle assessment: a case study in Tuscany, Italy. *Appl. Energy* 101, 103–111. <https://doi.org/10.1016/j.apenergy.2012.03.021>.
- Bauer, C., Hofer, J., Althaus, H.-J., Del Duce, A., Simons, A., 2015. The environmental performance of current and future passenger vehicles: life cycle assessment based on a novel scenario analysis framework. *Appl. Energy* 157, 871–883. <https://doi.org/10.1016/j.apenergy.2015.01.019>.
- Bento, N., 2016. 15 - investment in the infrastructure for hydrogen passenger cars—new hype or reality? *Woodhead Publ. Ser. Energy* 2, 379–409. <https://doi.org/10.1016/B978-1-78242-362-1.00015-8>.
- Brodrick, C.J., Lipman, T.E., Farshchi, M., Lutsey, N.P., Dwyer, H.A., Sperling, D., Gouse III, S.W., Harris, D.B., King, F.G., 2002. Evaluation of fuel cell auxiliary power units for heavy-duty diesel trucks. *Transp. Res. Part D Transp. Environ.* 7, 303–315. [https://doi.org/10.1016/S1361-9209\(01\)00026-8](https://doi.org/10.1016/S1361-9209(01)00026-8).
- Burnham, A., Wang, M., Wu, Y., 2006. Development and applications of GREET 2.7 — the transportation vehicle-cycle model (Argonne National Laboratory) <http://www.osti.gov/servlets/purl/898530-scVqHe/> (accessed 5 November 2023).
- Cai, K., Sun, C., Wang, H., Song, Q., Wang, C., Wang, P., 2022. The potential challenge for the effective GHG emissions mitigation of urban energy consumption: a case study of Macau. *Environ. Impact Assess. Rev.* 93, 106717. <https://doi.org/10.1016/j.eiar.2021.106717>.
- Capolongo, F., Carbonei, J., Saltelli, A., 2007. An effective screening design for sensitivity analysis of large models. *Environ. Model Softw.* 22, 1509–1518. <https://doi.org/10.1016/j.envsoft.2006.10.004>.
- Canada energy regulator, 2022. Market snapshot: How much CO₂ do electric vehicles, hybrids and gasoline vehicles emit? <https://www.cer-rec.gc.ca/en/data-analys> is/energy-markets/market-snapshots/2018/market-snapshot-how-much-co2-do-electric-vehicles-hybrids-gasoline-vehicles-emit.html (accessed 2 June 2024).
- Canadian Automobile Association: Alberta Motor Association, 2024. General Rules for Speed Limits in Alberta. <https://ama.ab.ca/articles/rules-for-speed-limits-alberta> (accessed 1 February 2024).
- Candelaresi, D., Valente, A., Iribarren, D., Dufour, J., Spazzafumo, G., 2021. Comparative life cycle assessment of hydrogen-fuelled passenger cars. *Int. J. Hydrol. Energy* 46, 35961–35973. <https://doi.org/10.1016/j.ijhydene.2021.01.034>.
- Chen, L., Wang, Y., Jiang, Y., Zhang, C., Liao, Q., Li, J., Wu, J., Gao, X., 2024. Life cycle assessment of liquid hydrogen fuel for vehicles with different production routes in China. *Energy* 299. <https://doi.org/10.1016/j.energy.2024.131472>.
- Colella, W.G., Jacobson, M.Z., Golden, D.M., 2005. Switching to a U.S. hydrogen fuel cell vehicle fleet: the resultant change in emissions, energy use, and greenhouse gases. *J. Power Sources* 150, 150–181. <https://doi.org/10.1016/j.jpowsour.2005.05.092>.
- Cox, B., Bauer, C., Mendoza Beltran, A., van Vuuren, D.P., Mutel, C.L., 2020. Life cycle environmental and cost comparison of current and future passenger cars under different energy scenarios. *Appl. Energy* 269, 115021. <https://doi.org/10.1016/j.apenergy.2020.115021>.
- Czerwinski, F., 2021. Current trends in automotive lightweighting strategies and materials. *Mater.* 14, 6631. <https://doi.org/10.3390/ma14216631>.
- Davis, M., Moronkeji, A., Ahiduzzaman, M., Kumar, A., 2020. Assessment of renewable energy transition pathways for a fossil fuel-dependent electricity-producing jurisdiction. *Energy Sustain. Dev.* 59, 243–261. <https://doi.org/10.1016/j.esd.2020.10.011>.
- De Vlieger, I., De Keukeleere, D., Kretzschmar, J.G., 2000. Environmental effects of driving behaviour and congestion related to passenger cars. *Atmos. Environ.* 34, 4649–4655. [https://doi.org/10.1016/S1352-2310\(00\)00217-X](https://doi.org/10.1016/S1352-2310(00)00217-X).
- Del Duce, A., Gauch, M., Althaus, H.J., 2016. Electric passenger car transport and passenger car life cycle inventories in ecoinvent version 3. *Int. J. Life Cycle Assess.* 21, 1314–1326. <https://doi.org/10.1007/s11367-014-0792-4>.
- Delucchi, M.A., Yang, C., Burke, A.F., Ogden, J.M., Kurani, K., Kessler, J., Sperling, D., 2014. An assessment of electric vehicles: technology, infrastructure requirements, greenhouse-gas emissions, petroleum use, material use, lifetime cost, consumer acceptance and policy initiatives. *Philos. Trans. R. Soc. A Math. Phys. Eng. Sci.* 372, 20120325. <https://doi.org/10.1098/rsta.2012.0325>.
- Di Lullo, G., Gemechu, E., Oni, A.O., Kumar, A., 2020. Extending sensitivity analysis using regression to effectively disseminate life cycle assessment results. *Int. J. Life Cycle Assess.* 25, 222–239. <https://doi.org/10.1007/s11367-019-01674-y>.
- Dincer, I., Rosen, M.A., 2011. Sustainability aspects of hydrogen and fuel cell systems. *Energy Sustain. Dev.* 15, 137–146. <https://doi.org/10.1016/j.esd.2011.03.006>.
- Dolweera, G., Hahn, F., Bergerson, J., Pruckner, M., 2020. A scenario-based study on the impacts of electric vehicles on energy consumption and sustainability in Alberta. *Appl. Energy* 268, 114961. <https://doi.org/10.1016/j.apenergy.2020.114961>.
- Ebaid, M.S.Y., Hammad, M., Alghamdi, T., 2015. THERMO economic analysis OF PV and hydrogen gas turbine hybrid power plant of 100 MW power output. *Int. J. Hydrol. Energy* 40, 12120–12143. <https://doi.org/10.1016/j.ijhydene.2015.07.077>.
- Egede, P., Dettmer, T., Herrmann, C., Kara, S., 2015. Life cycle assessment of electric vehicles – a framework to consider influencing factors. *Proc. CIRP* 29, 233–238. <https://doi.org/10.1016/j.procir.2015.02.185>.
- Ellingsen, L.A.W., Singh, B., Stromman, A.H., 2016. The size and range effect: life-cycle greenhouse gas emissions of electric vehicles. *Concawe Rev.* 2017, 6. <https://doi.org/10.1111/jiec.12072>.
- Environment Canada, 2014. Greenhouse Gas Sources and Sinks in Canada. <https://publications.gc.ca/site/eng/9.506002/publication.html> (accessed 5 November 2023).
- Faria, R., Moura, P., Delgado, J., De Almeida, A.T., 2012. A sustainability assessment of electric vehicles as a personal mobility system. *Energy Convers. Manag.* 61, 19–30. <https://doi.org/10.1016/j.enconman.2012.02.023>.
- Faria, R., Marques, P., Moura, P., Freire, F., Delgado, J., de Almeida, A.T., 2013. Impact of the electricity mix and use profile in the life-cycle assessment of electric vehicles. *Renew. Sust. Energ. Rev.* 24, 271–287. <https://doi.org/10.1016/j.rser.2013.03.063>.
- Fearnside, P.M., 2000. Why a 100-year time horizon should be used for global warming mitigation calculations. *Mitig. Adapt. Global Change* 7, 19–30. <https://doi.org/10.1023/A:1015885027530>.
- Garcia, R., Gregory, J., Freire, F., 2015. Dynamic fleet-based life-cycle greenhouse gas assessment of the introduction of electric vehicles in the Portuguese light-duty fleet. *Int. J. Life Cycle Assess.* 20, 1287–1299. <https://doi.org/10.1007/s11367-015-0921-8>.
- Ghirardi, E., Brumana, G., Franchini, G., Aristolao, N., Vedovati, G., 2024. The role of hydrogen storage and electric vehicles in grid-isolated hybrid energy system with high penetration of renewable. *Energy Convers. Manag.* 302. <https://doi.org/10.1016/j.enconman.2024.118154>.
- Ghosh, T., Kim, H.C., De Kleine, R., Wallington, T.J., Bakshi, B.R., 2021. Life cycle energy and greenhouse gas emissions implications of using carbon fiber reinforced polymers in automotive components: front subframe case study. *Sustain. Mater. Technol.* 28, e00263. <https://doi.org/10.1016/j.susmat.2021.e00263>.
- Giordano, G., Diaz-Londono, C., Grusso, G., 2023. Electric Vehicles. <https://ieeexplore.ieee.org/xel/7/8782711/889399/10274855.pdf> (accessed 5 November 2023).
- Glensor, K., María Rosa Muñoz, B., 2019. Life-cycle assessment of Brazilian transport biofuel and electrification pathways. *Sustainability* 11, 11226332. <https://doi.org/10.3390/su11226332>.
- Government of Canada, 2021. Urban mobility : Performance indicators, transport Canada. <https://tdih-edit.tc.canada.ca/libraries/pdf.js/web/viewer.html?file=https%3A%2F%2Ftdih-edit.tc.canada.ca%2Fsites%2Fdefault%2Ffiles%2F2022-08%2F232600012021001-eng.pdf> (accessed 31 January 2024).
- Government of Canada, 2024a. Historical Climate Data. https://climate.weather.gc.ca/index_e.html (accessed 31 January 2024).

- Government of Canada, 2024b. Historic data: Past weather and climate. https://climate.weather.gc.ca/historical_data/search_historic_data_e.html (accessed 31 January 2024).
- Greene, D.L., 2012. Rebound 2007: analysis of U.S. light-duty vehicle travel statistics. *Energy Policy* 41, 14–28. <https://doi.org/10.1016/j.enpol.2010.03.083>.
- Hawkins, T.R., Singh, B., Majeau-Bettez, G., Strømman, A.H., 2013. Comparative environmental life cycle assessment of conventional and electric vehicles. *J. Ind. Ecol.* 17. <https://doi.org/10.1111/j.1530-9290.2012.00532.x>.
- Hooftman, N., Messagie, M., Van Mierlo, J., Coosemans, T., 2018. A review of the European passenger car regulations – real driving emissions vs local air quality. *Renew. Sust. Energ. Rev.* 86, 1–21. <https://doi.org/10.1016/j.rser.2018.01.012>.
- Huang, Z., Zhang, X., 2006. Well-to-wheels analysis of hydrogen based fuel-cell vehicle pathways in Shanghai. *Energy* 31, 471–489. <https://doi.org/10.1016/j.energy.2005.02.019>.
- International Energy Agency, 2021. Global Hydrogen Review 2021. <https://www.iea.org/reports/global-hydrogen-review-2021> (accessed 5 February 2024).
- International organization for Standardization 14040:2006, 2022. Environmental management life cycle assessment principles and framework. <https://www.iso.org/standard/37456.html> (accessed 4 November 2023).
- Jochem, P., Babrowski, S., Fichtner, W., 2015. Assessing CO₂ emissions of electric vehicles in Germany in 2030. *Transp. Res. Part A Policy Pract.* 78, 68–83. <https://doi.org/10.1016/j.tra.2015.05.007>.
- Kalghatgi, G., 2018. Is it really the end of internal combustion engines and petroleum in transport? *Appl. Energy* 225, 965–974. <https://doi.org/10.1016/j.apenergy.2018.05.076>.
- Koffler, C., 2014. Life cycle assessment of automotive lightweighting through polymers under US boundary conditions. *Int. J. Life Cycle Assess.* 19, 538–545. <https://doi.org/10.1007/s11367-013-0652-7>.
- Koman, G., Kubina, M., Varmus, M., 2024. Electromobility in the world and in Slovakia. *Transp. Res. Proc.* 77, 224–230. <https://doi.org/10.1016/j.trpro.2024.01.030>.
- Koroma, M.S., Costa, D., Philippot, M., Cardellini, G., Hosen, M.S., Coosemans, T., Messagie, M., 2022. Life cycle assessment of battery electric vehicles: implications of future electricity mix and different battery end-of-life management. *Sci. Total Environ.* 831, 154859. <https://doi.org/10.1016/j.scitotenv.2022.154859>.
- Kukreja, B., 2008. Life cycle analysis of electric vehicles. https://sustain.ubc.ca/sites/default/files/2018-03%20Lifecycle%20Analysis%20of%20Electric%20Vehicles_Kukreja.pdf (accessed 5 November 2023).
- Kwon, S.Y., Park, J.Y., Kim, Y.J., 2020. Optimal V2G and route scheduling of mobile energy storage devices using a linear transit model to reduce electricity and transportation energy losses. *IEEE Trans. Ind. Appl.* 56, 34–47. <https://doi.org/10.1109/TIA.2019.2954072>.
- Lee, D.-Y., Elgawainy, A., Kotz, A., Vijayagopal, R., Marcinkoski, J., 2018. Life-cycle implications of hydrogen fuel cell electric vehicle technology for medium- and heavy-duty trucks. *J. Power Sources* 393, 217–229. <https://doi.org/10.1016/j.jpowsour.2018.05.012>.
- Lefèvre, J., Briand, Y., Pye, S., Tovilla, J., Li, F., Oshiro, K., Waisman, H., Cayla, J.-M., Zhang, R., 2021. A pathway design framework for sectoral deep decarbonization: the case of passenger transportation. *Clim. Pol.* 21, 93–106. <https://doi.org/10.1080/14693062.2020.1804817>.
- Li, B., Lv, X., Chen, J., 2024. Demand and supply gap analysis of Chinese new energy vehicle charging infrastructure: based on CNN-LSTM prediction model. *Renew. Energy* 220, 119618. <https://doi.org/10.1016/j.renene.2023.119618>.
- Lu, Y., Ge, Y., Chai, Y., 2022. Analysis of current situation, problems and potential solutions of electric vehicle industry. *Highlights Business, Econ. Manag.* 4, 11–16. <https://doi.org/10.54097/hbeam.v4i.3358>.
- Ma, H., Balthasar, F., Tait, N., Riera-Palou, X., Harrison, A., 2012. A new comparison between the life cycle greenhouse gas emissions of battery electric vehicles and internal combustion vehicles. *Energy Policy* 44, 160–173. <https://doi.org/10.1016/j.enpol.2012.01.034>.
- Marmiroli, B., Messagie, M., Dotelli, G., Van Mierlo, J., 2018. Electricity generation in LCA of electric vehicles: a review. *Appl. Sci.* 8, 1384. <https://doi.org/10.3390/app8081384>.
- Matheys, J., Timmermans, J.M., Van Mierlo, J., Meyer, S., Van Den Bossche, P., 2009. Comparison of the environmental impact of five electric vehicle battery technologies using LCA. *Int. J. Sustain. Manuf.* 1, 318–329. <https://doi.org/10.1504/IJSM.2009.023977>.
- Mayanti, B., 2024. Life cycle assessment of lithium iron phosphate and electrochemical recuperator cells for city buses in Finland. *Environ. Impact Assess. Rev.* 105, 107413. <https://doi.org/10.1016/j.eiar.2023.107413>.
- Milligan, R., 2017. Drive cycles for battery electric vehicles and their fleet management. In: Electric Vehicles: Prospects and Challenges. Elsevier, pp. 489–555. <https://doi.org/10.1016/B978-0-12-803021-9.00013-6>.
- Miotti, M., Hofer, J., Bauer, C., 2017. Integrated environmental and economic assessment of current and future fuel cell vehicles. *Int. J. Life Cycle Assess.* 22, 94–110. <https://doi.org/10.1007/s11367-015-0984-4>.
- Mohammed, A., Saif, O., Abo-Adma, M., Fahmy, A., Elazab, R., 2024. Strategies and sustainability in fast charging station deployment for electric vehicles. *Sci. Rep.* 14, 1–19. <https://doi.org/10.1038/s41598-023-50825-7>.
- Müller, M., Biedenbach, F., Reinhard, J., 2020. Development of an integrated simulation model for load and mobility profiles of private households. *Energies* 13, 13153843. <https://doi.org/10.3390/en13153843>.
- Nemry, F., Leduc, G., Mongelli, I., Uihlein, A., 2008. Environmental improvement of passenger cars (IMPRO-car). *JCR Sci. Tech. Reports EUR* 23038 EN. <https://doi.org/10.2791/63451>.
- Nigro, N., Jiang, S., 2013. Lifecycle greenhouse gas emissions from different light-duty vehicle pathways: A synthesis of recent research. <https://www.c2es.org/wp-content/uploads/2013/07/fuel-pathways-brief-07-19-13.pdf> (accessed 5 November 2023).
- Nikolaidis, P., Poulikkas, A., 2017. A comparative overview of hydrogen production processes. *Renew. Sust. Energ. Rev.* 67, 597–611. <https://doi.org/10.1016/j.rser.2016.09.044>.
- Nissan, 2019. Nissan Intelligent Mobility. <https://www.nissan.in/experience-nissan/nissan-intelligent-mobility.html> (accessed 5 November 2023).
- Onat, N.C., Kucukvar, M., 2022. A systematic review on sustainability assessment of electric vehicles: knowledge gaps and future perspectives. *Environ. Impact Assess. Rev.* 97, 106867. <https://doi.org/10.1016/j.eiar.2022.106867>.
- Onat, N.C., Kucukvar, M., Tatari, O., 2015. Conventional, hybrid, plug-in hybrid or electric vehicles? State-based comparative carbon and energy footprint analysis in the United States. *Appl. Energy* 150, 36–49. <https://doi.org/10.1016/j.apenergy.2015.04.001>.
- Oni, A.O., Anaya, K., Giwa, T., Di Lullo, G., Kumar, A., 2022. Comparative assessment of blue hydrogen from steam methane reforming, autothermal reforming, and natural gas decomposition technologies for natural gas-producing regions. *Energy Convers. Manag.* 254, 115245. <https://doi.org/10.1016/j.enconman.2022.115245>.
- Osborne, J., 2013. Automotive composites-in touch with lighter and more flexible solutions. *Met. Finish.* 111, 26–30. [https://doi.org/10.1016/S0026-0576\(13\)70159-4](https://doi.org/10.1016/S0026-0576(13)70159-4).
- Palazzo, J., Geyer, R., 2019. Consequential life cycle assessment of automotive material substitution: replacing steel with aluminum in production of north American vehicles. *Environ. Impact Assess. Rev.* 75, 47–58. <https://doi.org/10.1016/j.eiar.2018.12.001>.
- Patil, A., Patel, A., Purohit, R., 2017. An overview of polymeric materials for automotive applications. *Mater. Today Proc.* 4, 3807–3815. <https://doi.org/10.1016/j.mtpr.2017.02.278>.
- Peng, X., She, X., Li, C., Luo, Y., Zhang, T., Li, Y., Ding, Y., 2019. Liquid air energy storage flexibly coupled with LNG regassification for improving air liquefaction. *Appl. Energy* 250, 1190–1201. <https://doi.org/10.1016/j.apenergy.2019.05.040>.
- Peters, J.F., Baumann, M., Zimmermann, B., Braun, J., Weil, M., 2017. The environmental impact of Li-ion batteries and the role of key parameters – a review. *Renew. Sust. Energ. Rev.* 67, 491–506. <https://doi.org/10.1016/j.rser.2016.08.039>.
- Shao, T., Peng, T., Zhu, L., Lu, Y., Wang, L., Pan, X., 2024. China's transportation decarbonization in the context of carbon neutrality: a segment-mode analysis using integrated modelling. *Environ. Impact Assess. Rev.* 105, 1–14. <https://doi.org/10.1016/j.eiar.2023.107392>.
- Simons, A., Bauer, C., 2015. A life-cycle perspective on automotive fuel cells. *Appl. Energy* 157, 884–896. <https://doi.org/10.1016/j.apenergy.2015.07.001>.
- Smith, C., Huppmann, D., 2022. Mitigation pathways compatible with 1.5°C in the context of sustainable development, the intergovernmental panel on climate change <https://www.cambridge.org/core/books/global-warming-of-15c/frontmatter/F7A8197ED6B28A8840D13915A537AF68> (accessed 1 February 2024).
- Solar on EV, 2024. Worldwide daily driving distance is 25–50km? what about AU, US, UK, EU, and... <https://www.solaronev.com/post/average-daily-driving-distance-for-passenger-vehicles> (accessed 06 November 2023).
- Statistics Canada, 2009. Canadian vehicle survey : Annual. https://publications.gc.ca/collections/collection_2009/statcan/53F0004X/53f0004x2009002-eng.pdf (accessed 31 January 2024).
- Statistics Canada, 2019. Study: Long commutes to work by car. <https://www150.statcan.gc.ca/n1/daily-quotidien/190225/dq190225a-eng.htm> (accessed 31 January 2024).
- Staudinger, J., Keoleian, G.A., Flynn, M.S., 2001. Management of end-of life vehicles (ELVs) in the US. http://css.snr.umich.edu/css_doc/CSS01-01.pdf (accessed 5 November 2023).
- Stockholm Environment Institute, 2022. Low Emission Analysis Platform (LEAP). <https://www.sei.org/tools/leap-long-range-energy-alternatives-planning-system/> (accessed 1 February 2024).
- Tagliaferri, C., Evangelisti, S., Accocia, F., Domenech, T., Ekins, P., Barletta, D., Lettieri, P., 2016. Life cycle assessment of future electric and hybrid vehicles: a cradle-to-grave systems engineering approach. *Chem. Eng. Res. Des.* 112, 298–309. <https://doi.org/10.1016/j.cherd.2016.07.003>.
- Tang, J., Li, J., Ding, F., Li, Z., Wang, Y., Deng, F., 2017. Effects of different depth of discharge on cycle life of LiFePO₄ battery. *ECS. Meet. Abstr. MA2017-01*, 441. <https://doi.org/10.1149/ma2017-01/5/441>.
- Tao, Z., Zhao, L., Changxin, Z., 2011. Research on the prospects of low-carbon economic development in China based on LEAP model. *Energy Procedia* 5, 695–699. <https://doi.org/10.1111/j.1530-9290.2012.00532.x>.
- Temporelli, A., Carvalho, M.L., Girardi, P., 2020. Life cycle assessment of electric vehicle batteries: an overview of recent literature. *Energies* 13, 13112864. <https://doi.org/10.3390/en13112864>.
- Travel British Columbia, 2024. Road and Driving Information. <https://www.travel-british-columbia.com/travel-resources/transportation/road-driving-info/> (accessed 1 February 2024).
- Tutuiuan, M., Bonnel, P., Ciuffo, B., Haniu, T., Ichikawa, N., Marotta, A., Pavlovic, J., Steven, H., 2015. Development of the world-wide harmonized light duty test cycle (WLTC) and a possible pathway for its introduction in the European legislation. *Transp. Res. Part D Transp. Environ.* 40, 61–75. <https://doi.org/10.1016/j.trd.2015.07.011>.
- United Nations Climate Change, 2021. The Paris Agreement. <https://www.un.org/en/climatechange/paris-agreement> (accessed 5 November 2023).
- Wager, G., Whale, J., Braul, T., 2016. Driving electric vehicles at highway speeds: the effect of higher driving speeds on energy consumption and driving range for electric vehicles in Australia. *Renew. Sust. Energ. Rev.* 63, 158–165. <https://doi.org/10.1016/j.rser.2016.05.060>.

- Wang, H., Chen, C., Huang, C., Fu, L., 2008. On-road vehicle emission inventory and its uncertainty analysis for Shanghai, China. *Sci. Total Environ.* 398, 60–67. <https://doi.org/10.1016/j.scitotenv.2008.01.038>.
- Weis, A., Michalek, J.J., Jaramillo, P., Lueken, R., 2015. Emissions and cost implications of controlled electric vehicle charging in the U.S. PJM interconnection. *Environ. Sci. Technol.* 49, 5813–5819. <https://doi.org/10.1021/es505822f>.
- Wong, Y.Y.C., Ho, D.C.K., So, S., Tsang, C.W., Chan, E.M.H., 2021. Life cycle assessment of electric vehicles and hydrogen fuel cell vehicles using the GREET model—a comparative study. *Sustainability* 13, 13094872. <https://doi.org/10.3390/su13094872>.
- Wu, J., Li, Q., Liu, G., Xie, R., Zou, Y., Scipioni, A., Manzardo, A., 2022. Evaluating the impact of refrigerated transport trucks in China on climate change from the life cycle perspective. *Environ. Impact Assess. Rev.* 97, 106866. <https://doi.org/10.1016/j.eiar.2022.106866>.
- Zhang, R., Fujimori, S., 2020. The role of transport electrification in global climate change mitigation scenarios. *Environ. Res. Lett.* 15, 1748–9326. <https://doi.org/10.1088/1748-9326/ab6658>.
- Zhang, L., Qin, Q., 2018. China's new energy vehicle policies: evolution, comparison and recommendation. *Transp. Res. Part A Policy Pract.* 110, 57–72. <https://doi.org/10.1016/j.tra.2018.02.012>.
- Zhao, J., Xi, X., Na, Q., Wang, S., Kadry, S.N., Kumar, P.M., 2021. The technological innovation of hybrid and plug-in electric vehicles for environment carbon pollution control. *Environ. Impact Assess. Rev.* 86. <https://doi.org/10.1016/j.eiar.2020.106506>.
- Zheng, C., Wei, Xiao, Z., Niu, Peng, Y., Hua, Li, C., Yin, Du, Z., Bo, 2018. Rezoning global offshore wind energy resources. *Renew. Energy* 129, 1–11. <https://doi.org/10.1016/j.renene.2018.05.090>.